agriculture

MDPI

Article

Bacillus velezensis B313-6 as a Potential Biocontrol Strain Against Anthracnose of *Panax quinquefolius*, and Its Fermentation Optimization, and Field Efficacy on American Ginseng

Shuang Feng [1], Yue Shi [1], Ruijie Liu [1], Xin Li [1], Shuai Shao [1], Nan Yin [1], Yuejia Song [1], Haoxin Zhan [1], Yuxin He [1], Tom Hsiang [2], Changqing Chen [1], Liping Liu [1,*] and Jie Gao [3,*]

[1] College of Plant Protection, Jilin Agricultural University, Changchun 130118, China
[2] School of Environmental Sciences, University of Guelph, Guelph, ON N1G 2W1, Canada
[3] State-Local Joint Engineering Research Center of Ginseng Breeding and Application, Changchun 130118, China
* Correspondence: lipingl@jlau.edu.cn (L.L.); jiegao115@jlau.edu.cn (J.G.)

Abstract

Anthracnose of American ginseng is caused by *Colletotrichum panacicola*. In this study, *Bacillus velezensis* B313-6, isolated from the rhizosphere soil of American ginseng, was identified based on morphological, physiological, biochemical, 16S rRNA, and the gyrase subunit A protein (*gyrA*) regions' analyses. *B. velezensis* B313-6 showed strong antagonistic activity against *C. panacicola* with an inhibition rate of 94.4% in dual culture assay, and exhibited broad-spectrum antifungal activity against eight other plant pathogenic fungi (inhibition rates 70–94%). Using single-factor experiments combined with response surface methodology, the fermentation conditions were optimized, increasing the inhibition rate against *C. panacicola* from 93.9% to 97.4%. In field trials, the *B. velezensis* B313-6 fermentation broth at a low dose (33.3 mL/m^2) provided a control efficacy of 67.6% after the third spray, comparable to a commercial *B. subtilis* product used as a positive control. The low-dose treatment also significantly promoted American ginseng growth, increasing plant height, root length, shoot fresh weight and root fresh weight by 9.7%, 11.3%, 10.5% and 15.5%, respectively, compared to the treatment of water. These results indicate that *B. velezensis* B313-6 has great potential as a biocontrol agent against the anthracnose of *Panax quinquefolius* and also promotes the growth of American ginseng.

Keywords: *Bacillus velezensis*; American ginseng anthracnose; *Colletotrichum panacicola*; biological control; fermentation optimization; field efficacy

Check for updates

Academic Editor: Giuseppe Lima

Received: 18 June 2026
Revised: 28 July 2026
Accepted: 1 August 2026
Published: 4 August 2026

Copyright: © 2026 by the authors. Licensee MDPI, Basel, Switzerland. This article is an open access article distributed under the terms and conditions of the Creative Commons Attribution (CC BY) license.

1. Introduction

Panax quinquefolius L. (American ginseng) is a perennial herbaceous plant in the family Araliaceae. Its roots are rich in saponins, which have been reported to exhibit notable effects in anti-fatigue, immune enhancement, and cardiovascular function regulation, contributing to its high economic value as a medicinal plant [1]. This crop is widely cultivated in Northeast China and has become an economically important crop for local farmers [2,3]. However, the anthracnose caused by *Colletotrichum panacicola* is one of the most severe leaf diseases in ginseng or American ginseng production [4,5]. Anthracnose caused by *Colletotrichum panacicola* is a destructive disease affecting *Panax ginseng* and *P. quinquefolius* at all growth stages, damaging leaves, stems, and seeds, and leading to

significant yield losses [4,5]. In recent years, its incidence has increased in major ginseng-producing regions of Northeast China, such as Tonghua and Dunhua City [5]. In early stages, it causes nearly circular or elliptical brown lesions on leaves, stems, or seeds. Under severe conditions, lesions coalesce and cause leaf blight (such as on leaves), which severely inhibits photosynthesis and ultimately leads to a significant reduction in yield and quality. In field production, chemical fungicides are commonly used for disease management [6]. However, long-term and excessive application not only induces pathogen resistance and reduces control efficacy, but also leads to fungicide residues that contaminate soil and water, accumulate in the medicinal material, and threaten both human safety and the ecological environment [7–10]. Moreover, the cultivation period of American ginseng lasts 3–5 years, and continuous fungicide application further disrupts the soil microecology and aggravates continuous cropping obstacles [11]. Therefore, developing green and safe alternative control technologies is an urgent need to ensure the sustainable development of the ginseng industry. Biological control, which uses beneficial microorganisms and their metabolites to suppress pathogens, offers advantages such as a generally lower risk of resistance development, reduced environmental impact, and compatibility with organic farming [12].

Bacillus velezensis is widely distributed in the environment. Approximately 5–8% of its protein-coding genes are involved in the synthesis of antimicrobial compounds, including hydrolases, volatile compounds, bacteriocins, polyketides, and lipopeptides [13,14]. Its biocontrol mechanism is not based solely on direct pathogen inhibition. Instead, it acts through multiple synergistic pathways, including direct antagonism of pathogens, induction of systemic resistance in plants, and regulation of rhizosphere microecology [15–17].

Full exploitation of the biocontrol potential of a microbial strain depends on an efficient fermentation process. Microbial growth and metabolite production are highly strain-specific. Nutrient supply and culture environment directly affect physiological activity, and therefore, optimizing the composition of the fermentation medium and the cultivation parameters is a critical step in the development of biocontrol agents [18]. Such optimization not only enhances cell biomass and viable cell counts but also maximizes the yield of secondary metabolites with antimicrobial activity, ensuring a stable and effective final product. Fermentation performance is governed by multiple factors, including carbon and nitrogen sources, temperature, pH, inoculum size, and agitation speed, all of which can significantly affect bacterial growth, sporulation, and the synthesis of bioactive compounds [19]. To systematically address this multivariable complexity, Response Surface Methodology (RSM) has emerged as a powerful statistical and mathematical tool for modeling and optimizing processes in which a response of interest is influenced by several independent variables. Unlike the traditional one-factor-at-a-time approach, which fails to detect interactions between factors, or orthogonal array designs, which are limited in their predictive capability, RSM establishes a quantitative empirical model that elucidates both the individual and interactive effects of multiple parameters [20,21]. This enables the identification of optimal conditions with a substantially reduced number of experimental runs, offering both efficiency and accuracy. Previous studies have confirmed that integrating single-factor experiments with RSM to optimize the fermentation process of *B. velezensis* could significantly enhance the antifungal activity of the resulting fermentation broth [22,23].

In this study, a plate confrontation assay was employed to screen rhizosphere soil of American ginseng for biocontrol strains with strong activity against *C. panacicola* [24]. We sought to identify a highly effective antagonistic strain and evaluate its antifungal spectrum, optimize its fermentation conditions for enhanced production of antifungal metabolites, and verify its in situ control efficacy and growth-promoting effects on American ginseng

through field trials. This study aims to provide a promising biocontrol strain for the green management of American ginseng anthracnose, along with optimized fermentation parameters, to support the development of more sustainable disease control strategies for this important medicinal crop.

2. Materials and Methods

2.1. Source and Screening of the Antagonistic Strain

The bacterial strains used in this study were previously isolated from the rhizosphere soil of healthy American ginseng plants in Jilin and Heilongjiang provinces. A 10 g soil sample was suspended in 90 mL of sterile water and shaken at 180 rpm for 30 min at 28 °C to prepare a soil suspension. The suspension was serially diluted 10-fold, and 100 µL aliquots of the 10^{-4}, 10^{-5}, and 10^{-6} dilutions were spread onto nutrient agar (NA) plates, followed by incubation at 28 °C for 24–48 h. Single colonies with distinct morphological characteristics were picked and purified by repeated streaking. A total of 132 bacterial isolates were obtained and maintained in the culture collection of the Laboratory of Green Fungi Management for Medicinal Plants, Jilin Agricultural University. These strains were subjected to preliminary screening for antagonistic activity against *C. panacicola*, the causal agent of American ginseng anthracnose, using a dual culture assay. A 8-mm diameter mycelial plug of the target pathogen was placed in the center of a PDA plate, and 20 µL of the test bacterial suspension (OD_{600} = 1.0) were added at equal distances on both sides of the plug. After incubation at 25 °C for 5–7 days, the colony diameter of the pathogen was measured, and the inhibition rate was calculated according to this formula: Inhibition rate (%) = (Control colony diameter − Treatment colony diameter)/(Control colony diameter − Mycelial disk diameter) × 100. Each treatment was performed in three independent biological replicates, with three technical replicates per replicate. Strains showing more than 70% inhibition in the dual culture assay were defined as potential highly active antagonists [25].

2.2. Identification of the Antagonistic Strain B313-6

2.2.1. Morphological Identification

The strain B313-6 was streak-inoculated onto nutrient agar (NA) and incubated at 28 °C for 24–48 h. Colony characteristics (size, shape, color, margin, surface gloss, and transparency) were observed. Cells from the logarithmic growth phase were Gram-stained and examined under a light microscope for cell morphology and staining reaction. Gram-positive cells appear purple, while Gram-negative cells appear red.

2.2.2. Physiological and Biochemical Tests

Physiological and biochemical tests were performed according to Bergey's Manual of Determinative Bacteriology [26]. The tests included salt tolerance (2%, 5%, 7%, 10%, *w*/*v*), glucose oxidation-fermentation, nitrate reduction, nitrite reduction, gelatin liquefaction, citrate utilization, malonate utilization, starch hydrolysis, fluorescent pigment production, phenylalanine deaminase, Voges–Proskauer (V–P) test, methyl red test, and carbon source utilization (glucose, sucrose, fructose, xylose, maltose, mannitol, trehalose, lactose).

2.2.3. Molecular Identification

Total DNA of the strain B313-6 was extracted using a bacterial genomic DNA extraction kit (Tiangen Biotech, Beijing, Co., Ltd., Beijing, China). The 16S rRNA gene was amplified by PCR using the universal primers 27F (5′-AGAGTTTGATCCTGGCTCAG-3′) and 1492R (5′-GGTTACCTTGTTACGACTT-3′). To further confirm the species identification, the sequence of *gyrA* was amplified using the primers *gyrA*-F (5′-CAGTCAGGAAATGCGTACGTCCTT-3′)

and *gyrA*-R (5′-CAAGGTAATGCTCCAGGCATTGCT-3′). The PCR reaction mixture (20 μL) contained 1 μL of template DNA, 1 μL each of forward and reverse primers (10 μmol/L), 7 μL of 2× Magic Green Taq SuperMix, and ddH_2O to bring the volume to 20 μL. The amplification program was as follows: initial denaturation at 95 °C for 3 min; then 35 cycles of denaturation at 95 °C for 10 s, annealing at 56 °C for 10 s, and extension at 72 °C for 90 s; followed by a final extension at 72 °C for 5 min. The PCR products were verified by 1% agarose gel electrophoresis and sequenced. The obtained 16S rRNA and *gyrA* sequences were compared using BLASTn against the NCBI database. Reference sequences of closely related species within the genus *Bacillus*, particularly those from the *B. subtilis* group, were selected based on the highest BLAST similarity scores and included type strains of each species. Multiple sequence alignment was performed using Clustal W in MEGA 11. Phylogenetic trees were constructed separately based on the 16S rRNA and *gyrA* sequences using the neighbor-joining (NJ) method with the Kimura 2-parameter model as the distance metric. Tree topology was inferred using the nearest-neighbor interchange (NNI) algorithm. Gaps were treated with pairwise deletion. Bootstrap analysis with 1000 replicates was performed to assess the reliability of the branching patterns [27–29]. For the tree of the 16S rRNA sequence, *B. pumilus* ATCC 7061^T (NR043242) was used as the outgroup, and for the tree of *gyrA* sequence, *B. pumilus* ATCC 7061^T (EU138655) was used as the outgroup.

2.3. Determination of Antagonistic Spectrum

The antagonistic activity of *B. velezensis* B313-6 against eight common phytopathogenic fungi was evaluated using the plate confrontation method. The tested fungi were: *Botrytis cinerea*, *C. orbiculare*, *Fusarium graminearum*, *F. oxysporum* (on maize), *F. oxysporum* f. sp. *ginseng* (on ginseng), *Sclerotinia nivalis*, *Ilyonectria robusta*, and *Rhizoctonia solani*. All fungal isolates used in the antifungal spectrum assay were obtained from the culture collection of the College of Plant Protection Research, Jilin Agricultural University (deposited as the CCR collection). These isolates were previously identified based on morphological characteristics and molecular methods (ITS or other phylogenetic markers), and the relevant references are provided from our study teams [30–32].

Each pathogenic fungus was sub-cultured on PDA plates at 25 °C for 5–7 days from long term stock. A mycelial plug of 8 mm in diameter was taken with a cork borer and placed in the center of a fresh PDA plate. Two 6-mm-diameter plugs were taken from the PDA at 2 cm from both sides of the fungal inoculum plug, and 20 μL of the bacterial suspension of *B. velezensis* B313-6 (OD_{600} = 1.0) was injected into each hole. Plates without the antagonistic bacterium were used as controls. Each treatment had three replicates. After incubation at 25 °C for 5–7 days, when the fungal colonies had fully grown, the colony diameters of the fungi in each treatment were measured, and the inhibition rate was calculated following the formula above.

2.4. Optimization of Fermentation Conditions

2.4.1. Seed Culture and Screening of Basal Medium

Since the initial inhibition rate of *B. velezensis* B313-6 against *C. panacicola* had already reached a high level, it was not suitable as a sensitive indicator for detecting incremental improvements during the optimization process. Therefore, OD_{600} was used as the response variable to guide the optimization of fermentation conditions. A single colony of *B. velezensis* B313-6 was inoculated into LB liquid medium and cultured at 28 °C with shaking at 180 rpm for 12 h to obtain a seed culture. The seed culture was then inoculated (2%, *v*/*v*) into five different basal media: LB (Luria–Bertani), NB (Nutrient Broth), CM (Complex Medium), YSP (Yeast extract Sucrose Peptone), and NYBD (Nutrient Yeast Broth with Dextrose). The cultures were incubated at 28 °C and 180 rpm for 24 h. After incubation,

the OD_{600} of each fermentation broth was measured, and the inhibition rate against *C. panacicola* was assessed by the plate confrontation method. The optimal basal medium was selected based on both parameters. Each treatment was performed in triplicate.

2.4.2. Single-Factor Optimization of Medium Components and Culture Conditions

Based on the basal medium identified, single-factor experiments were conducted to optimize the medium amendments and culture conditions. In all experiments, OD_{600} was used as the response value, and each treatment had three replicates.

(1) Carbon source optimization. The carbon source in the basal medium was replaced individually with equal masses (20 g/L) of fructose, lactose, soluble starch, glucose, maltose, corn flour, sorbitol, or dextrin. The optimal carbon source was determined. After that, a concentration gradient (10, 15, 20, 25, 30 g/L) was tested to find the optimal concentration.

(2) Nitrogen source optimization. Based on the optimal carbon source, the nitrogen source was replaced individually with equal masses (15 g/L) of yeast extract, beef extract, soybean meal, urea, tryptone, ammonium chloride, ammonium sulfate, or ammonium nitrate. The optimal nitrogen source was identified, and its optimal concentration was determined (10, 15, 20, 25, 30 g/L).

(3) Inorganic salt optimization. Based on the optimal carbon and nitrogen sources, the inorganic salt content was replaced individually with equal masses (5 g/L) of potassium chloride, magnesium sulfate heptahydrate, potassium dihydrogen phosphate, calcium carbonate, potassium nitrate, manganese sulfate monohydrate, ferrous sulfate heptahydrate, or zinc sulfate heptahydrate. The optimal inorganic salt was selected, and its optimal concentration was determined (1, 2, 3, 4, 5 g/L).

(4) Culture condition optimization. Using the optimized medium, the following parameters were sequentially tested: size concentration (1%, 2%, 3%, 4%, 5%, 6%), broth volume (25, 50, 75, 100, 125 mL in a 250 mL flask), initial pH (5.0, 6.0, 7.0, 8.0, 9.0), temperature (24, 26, 28, 30, 32 °C), shaking speed (140, 160, 180, 200, 220 rpm), and fermentation time (12, 24, 36, 48, 60 h). The effect on OD_{600} was measured for each condition.

2.4.3. Plackett-Burman Screening of Key Factors

A Plackett–Burman design with $n = 12$ was used to evaluate the significance of the following nine factors: glucose concentration (2.0% and 2.5%), tryptone concentration (1.0% and 2.0%), KCl concentration (0.1% and 0.2%), size concentration (1% and 5%), liquid volume (50 and 125 mL in a 250 mL flask), initial pH (6.0 and 9.0), incubation temperature (24 and 30 °C), shaking speed (140 and 160 rpm), and fermentation time (12 and 24 h). OD_{600} was used as the response value. All experimental designs and regression analyses were performed using Design-Expert software (Version 13.0, Stat-Ease Inc., Minneapolis, MN, USA). The significance of each factor was determined by Student's *t*-test on the regression coefficients, and the model was evaluated by analysis of variance (ANOVA). Each experimental group had three replicates.

Notably, the Plackett–Burman design with 12 runs and nine factors is inherently a screening design, intended to identify the most influential factors from a relatively large set of variables with minimal experimental effort. While the design provides limited degrees of freedom for estimating experimental error, this is a recognized feature of this approach, and the significance of each factor was evaluated by ANOVA (factors with $p < 0.05$ were considered significant). Importantly, the reliability of the identified key factors was further validated through subsequent steepest ascent experiments and response surface optimization, confirming that the screening results were effective and reproducible.

2.4.4. Steepest Ascent Experiment

From the Plackett-Burman results, the effect coefficient and direction for each significant factor were obtained. Step sizes and the ascent direction were determined according to the effect coefficients. A steepest ascent experiment was then performed, and the center point for subsequent response surface analysis was selected based on the OD_{600} values. Each experimental group had three replicates.

2.4.5. Box–Behnken Response Surface Optimization

Using the center point obtained from the steepest ascent experiment, a Box–Behnken design with three factors and three levels was applied to optimize the three key factors. The response variable (Y) was OD_{600}. A second-order quadratic model was fitted to the experimental data by multiple regression analysis using the least-squares method in Design-Expert 13.0. The significance of the model terms was evaluated by ANOVA, and the optimal conditions were predicted by the software's numerical optimization function. Each experimental group had three replicates.

2.4.6. Validation of Optimized Conditions

Fermentation was conducted under the optimal conditions predicted by the response surface model. The initial (unoptimized) conditions (LB medium, size concentration 2%, broth volume 100 mL/250 mL, 28 °C, 180 rpm, 24 h) served as the control. OD_{600} and the inhibition rate against *C. panacicola* were measured for both the optimized and control fermentation broths. Each treatment had three replicates.

2.5. Field Efficacy, Growth-Promoting Effects, and Rhizosphere Microbiome Analysis

2.5.1. Field Experiment and Agronomic Trait Measurements

The field experiment was conducted in 2024 at an American ginseng plantation in Taiwang Town, Ji'an City, Jilin Province, China. Four treatments were set: (1) low-dose *B. velezensis* B313-6 fermentation broth (5×10^8 CFU/mL) at 33.3 mL/m^2; (2) high-dose fermentation broth (10 times the low dose) at 333.3 mL/m^2; (3) positive control: *Bacillus subtilis* commercial wettable powder (*B. subtilis* CWP, 1000 billion spores/g; Wuhan Kenuo Biotechnology Co., Ltd., Wuhan, China) at 0.8 g/m^2; and (4) water control. Each treatment had three replicates, with a plot area of 1.5 m^2 arranged in a randomized complete block design. The first application was performed at the early stage of disease development; disease incidence was recorded before application as the baseline. The suspensions were sprayed uniformly, with applications repeated every 10 days for a total of three applications. Ten days after the final application, disease incidence was assessed in each plot using a five-point sampling method. Disease severity was graded as follows: 0 = no lesion; 1 = lesion area covering 1–5% of leaf area; 3 = 5.1–10%; 5 = 10.1–20%; 7 = 20.1–50%; 9 = 51–100%. Based on this scale, the disease index and field control efficacy were calculated. The raw severity scores were used to calculate the disease index, and all statistical comparisons were performed on the disease index values using non-parametric methods. For each plot, ten randomly selected plants were harvested for agronomic trait measurement. Plant height was measured from the soil surface to the highest point of the longest leaf using a ruler. Root length was measured from the root crown to the tip of the longest root. Above-ground fresh weight (stems and leaves) and root fresh weight were determined immediately after harvest using an electronic balance after gently removing large soil particles [33,34].

$$\text{Disease index} = [\Sigma\ (\text{Disease rating} \times \text{Number of leaves with that rating})/(9 \times \text{Total number of leaves examined})] \times 100$$

$$\text{Control efficacy (\%)} = (\text{Disease index of control} - \text{Disease index of treatment})/\text{Disease index of control} \times 100$$

2.5.2. Rhizosphere Soil Sampling and Microbiome Analysis

After the final treatment application, rhizosphere soil samples were collected from each plot. Soil loosely adhering to the roots was gently removed, and the remaining rhizosphere soil tightly attached to the root surface was collected using a sterile brush. The soil samples were passed through a 2 mm sieve and stored at −80 °C. The samples were then shipped to Novogene Co., Ltd. (Beijing, China) for DNA extraction, library construction, and sequencing on an Illumina NovaSeq 6000 platform. The fungal ITS2 region was sequenced. Bioinformatic analysis was performed using UPARSE for OTU clustering at 97% sequence identity. Taxonomic assignment was conducted using the UNITE database for fungi. Relative abundances of fungal taxa at the genus level were calculated for each sample.

2.6. Statistical Analysis

All experimental data were expressed as mean ± standard deviation [35]. For disease index data, which were derived from ordinal severity scores, differences among treatments were analyzed using the Kruskal–Wallis non-parametric test, followed by Dunn's post hoc test with Bonferroni correction. For other continuous variables (plant height, root length, and fresh weights), one-way analysis of variance (ANOVA) was performed using SPSS 27.0 software. Differences between treatments were evaluated by Duncan's new multiple range test, with a significance level set at $p < 0.05$. Normality and homogeneity of variances for these continuous variables were confirmed using Shapiro–Wilk and Levene's tests prior to ANOVA. The design and data analysis for response surface optimization were carried out using Design-Expert 13 software. Graphs were prepared with Origin 2021 software.

3. Results

3.1. Identification of B. velezensis B313-6

Among the 132 bacterial isolates tested, *B. velezensis* B313-6 showed an inhibition rate of (94.4 ± 0.4) % against *C. panacicola* in the dual culture assay. After 48 h of culture on NA medium, *B. velezensis* B313-6 formed white colonies with irregular edges. The colony surface was smooth at the early stage but became slightly convex in the center at the later stage (Figure 1A). Gram staining was positive, and the cells were rod-shaped with blunt, rounded ends (Figure 1B). The physiological and biochemical identification results are shown in Table 1. *B. velezensis* B313-6 tested positive for starch hydrolysis, gelatin liquefaction, nitrate reduction, and the Voges–Proskauer (V–P) test; its glucose oxidation fermentation was fermentative. It grew in media containing 2%, 5%, 7%, and 10% NaCl. The following tests were negative: phenylalanine deaminase, indole production, methyl red, citrate utilization, malonate utilization, nitrite reduction, and fluorescent pigment production. Carbon source utilization tests showed that the strain could use glucose, maltose, mannitol, lactose, sucrose, trehalose, fructose, and xylose.

The 16S rRNA and *gyrA* gene sequences of *B. velezensis* B313-6 were amplified and analyzed. BLASTn analysis of the 16S rRNA and *gyrA* gene sequences showed the highest similarity to sequences belonging to the *Bacillus velezensis* group. Phylogenetic trees constructed separately based on the 16S rRNA and *gyrA* gene sequences (Figure 1C,D) consistently placed *B. velezensis* B313-6 within the clade containing *B. velezensis* with high bootstrap support. Based on morphological, physiological, biochemical characteristics, and molecular analyses (16S rRNA and *gyrA* sequencing), *B. velezensis* B313-6 was identified as *B. velezensis*. This strain has been deposited in the China General Microbiological Culture Collection Center (CGMCC) under accession number CGMCC 31782, and its 16S rRNA gene sequence has been assigned GenBank accession number PZ350614.

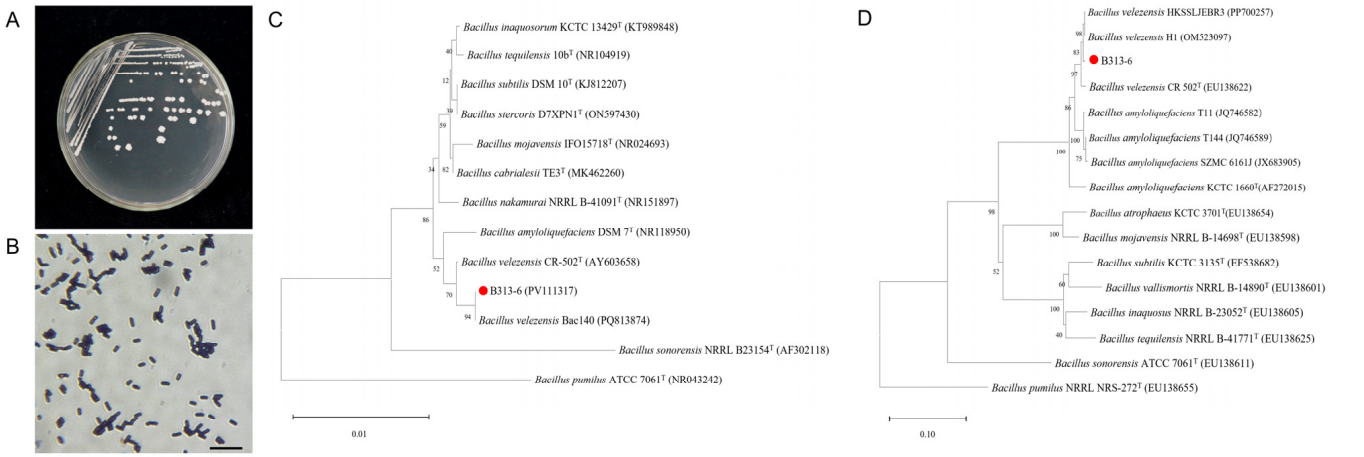


Figure 1. Morphological and phylogenetic characteristics of *Bacillus velezensis* B313-6. (**A**) Colony morphology of *B. velezensis* B313-6 on NA medium after 48 h of incubation. The colonies were white with irregular edges, smooth surface at the early stage, and slightly convex in the center at the later stage. (**B**) Gram staining of *B. velezensis* B313-6 showing rod-shaped cells with blunt, rounded ends (positive stain). (**C**) Neighbor-joining phylogenetic tree based on 16S rRNA gene sequences showing the relationship between *B. velezensis* B313-6 and related species. Bootstrap values (1000 replicates) are shown at branch nodes. The scale bar represents 0.01 substitutions per nucleotide position. (**D**) Neighbor-joining phylogenetic tree based on *gyrA* sequences showing the relationship between *B. velezensis* B313-6 and related species. Bootstrap values (1000 replicates) are shown at branch nodes. The scale bar represents 0.01 substitutions per nucleotide position. *B. velezensis* B313-6 was highlighted in the phylogenetic tree by adding a red solid circle (●) adjacent to it, as now shown in (**C**,**D**). Scale bars: 10 μm.

Table 1. Physiological and biochemical characterization of *Bacillus velezensis* B313-6.

Test Item	Result	Test Item	Result
Gram staining	+	Fluorescent pigment test	−
Salt tolerance		Phenylalanine deaminase test	−
2%	+	V–P test	+
5%	+	Methyl red test	−
7%	+	Carbon source utilization	
10%	+	Glucose	+
Glucose oxidative fermentation	fermentative	Sucrose	+
Nitrate reduction	+	Fructose	+
Nitrite reduction test	−	Xylose	+
Gelatin hydrolysis	+	Maltose	+
Citrate test	−	Mannitol	+
Malonate test	−	Trehalose	+
Starch hydrolysis	+	Lactose	+

Note: (+) Positive. (−) Negative.

3.2. Antagonistic Spectrum of B. velezensis B313-6

The results showed that this strain exhibited broad-spectrum antifungal activity. Among them, the highest inhibition rate, over 90%, was against *C. orbiculare*. The inhibition rates against seven other pathogens, and they all exceeded 70% (Table 2, Figure 2).

Table 2. Antifungal spectrum of *Bacillus velezensis* B313-6 against eight plant pathogenic fungi.

Pathogen	Host	Antifungal Rates (%)	Reference
Botrytis cinerea	*Panax ginseng*	84.19 ± 2.04	Liu et al. (2024) [30]
Colletotrichum orbiculare	*Cucumis sativus*	94.57 ± 1.10	this study
Fusarium graminearum	*Glycine max*	85.85 ± 1.52	this study
F. oxysporum	*Zea mays*	76.17 ± 0.90	Wang et al. (2022) [31]
F. oxysporum f. sp. *ginseng*	*P. ginseng*	77.21 ± 2.13	Wang et al. (2022) [31]
Ilyonectria robusta	*P. ginseng*	72.19 ± 1.85	Liu et al. (2024) [30]
Rhizoctonia solani	*P. ginseng*	85.38 ± 2.16	Liu et al. (2024) [30]
Sclerotinia nivalis	*P. ginseng*	73.88 ± 2.59	Feng et al. (2023) [32]

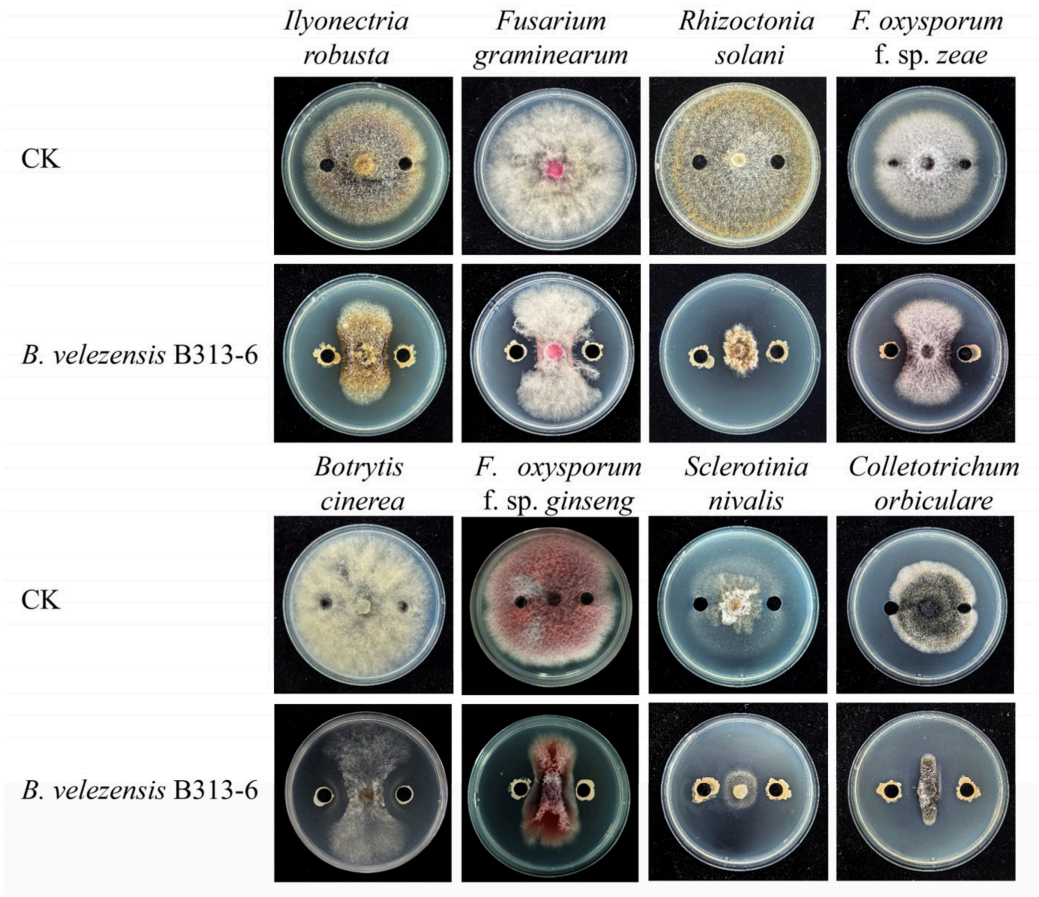


Figure 2. Antifungal spectrum of *Bacillus velezensis* B313-6 against eight common plant pathogenic fungi. Dual culture assays showing the antifungal activity of *B. velezensis* B313-6 against eight plant pathogenic fungi after 5–7 days of incubation (*B. cinerea*: 5 days; other seven pathogens: 7 days). The tested pathogens are indicated below each plate. Clear inhibition zones were observed around the bacterial spots. The corresponding inhibition rates are listed in Table 2.

3.3. Optimization of Fermentation Conditions of B. velezensis B313-6

3.3.1. Screening of Basal Medium

Bacillus velezensis B313-6 was inoculated into five liquid media and cultured at 28 °C and 180 rpm for 24 h, after which OD_{600} was measured. The results are shown in Figure 3A. The strain grew best in YSP medium, with an OD_{600} of 1.21, which was significantly higher than that in the other media ($p < 0.05$). Therefore, YSP was selected as the basal medium for subsequent optimization.

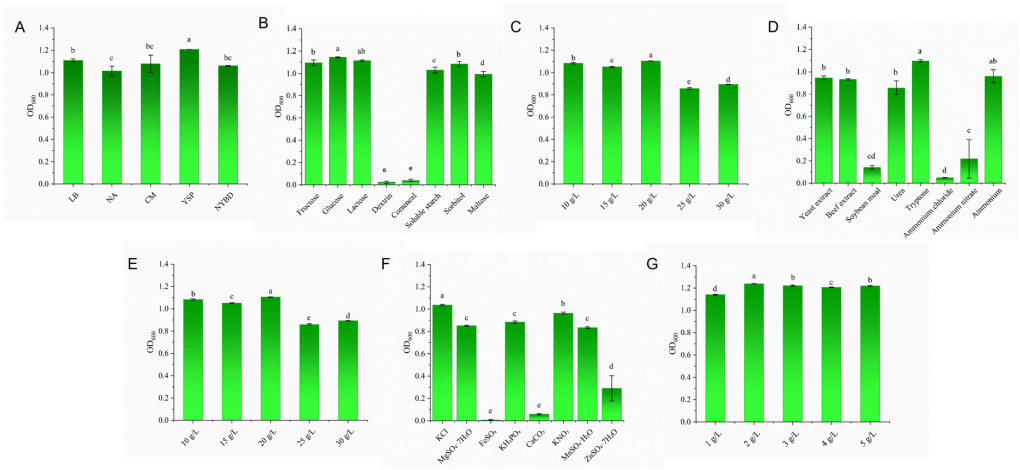


Figure 3. Optimization of basal medium and nutrient components (carbon source, nitrogen source, and inorganic salt) for *Bacillus velezensis* B313-6. Optimization of basal medium and nutrient components for *B. velezensis* B313-6. (**A**) Comparison of five basal media (LB, NB, CM, YSP, NYBD); YSP was the best. (**B**) Carbon source screening: glucose was optimal. (**C**) Glucose concentration optimization: 20 g/L was optimal. (**D**) Nitrogen source screening: tryptone was optimal. (**E**) Tryptone concentration optimization: 20 g/L was optimal. (**F**) Inorganic salt screening: KCl was optimal. (**G**) KCl concentration optimization: 2 g/L was optimal. Data are mean ± SD (n = 3). Different lowercase letters indicate significant differences ($p < 0.05$).

3.3.2. Single-Factor Optimization

Single-factor experiments were conducted to optimize the medium components and culture conditions. The results showed that the optimal carbon source was glucose (OD_{600} = 1.14, Figure 3B), and its optimal concentration was 20 g/L (OD_{600} = 1.10, Figure 3C). The optimal nitrogen source was tryptone (OD_{600} = 1.23, Figure 3D), with an optimal concentration of 20 g/L (OD_{600} = 1.29, Figure 3E). The optimal inorganic salt was KCl (OD_{600} = 1.04, Figure 3F), and its optimal concentration was 2 g/L (OD_{600} = 1.24, Figure 3G). The highest OD_{600} was achieved with a size concentration of 5% (1.25, Figure 4A), a liquid volume of 50 mL in a 250 mL flask (1.21, Figure 4B), an initial pH of 6.0 (1.22, Figure 4C), an incubation temperature of 30 °C (1.19, Figure 4D), a shaking speed of 160 rpm (1.18, Figure 4E), and a fermentation time of 24 h (1.20, Figure 4F).

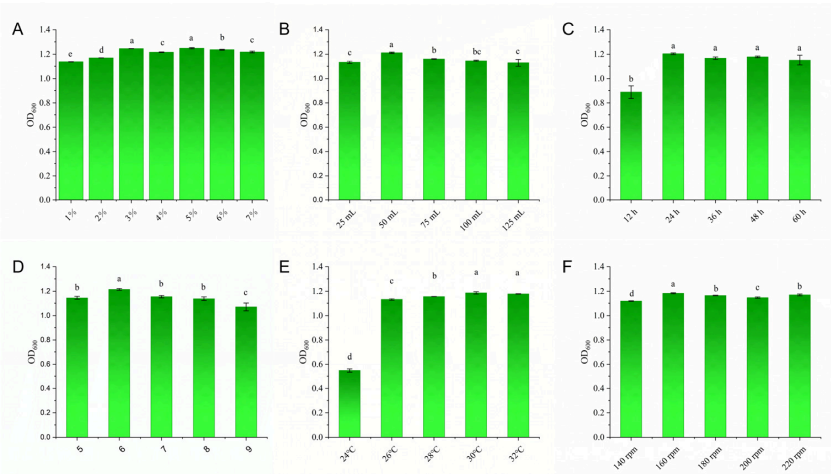


Figure 4. Optimization of culture conditions for *Bacillus velezensis* B313-6 by single-factor experiments. Optimization of culture conditions. (**A**) Inoculum size (5% optimal). (**B**) Liquid volume (50 mL/250 mL optimal). (**C**) Initial pH (6.0 optimal). (**D**) Temperature (30 °C optimal). (**E**) Shaking speed (160 rpm optimal). (**F**) Fermentation time (24 h optimal). Data are mean ± SD. Different lowercase letters indicate significant differences ($p < 0.05$).

3.3.3. Key Factors Identified by the Plackett-Burman Screening

Based on the single-factor experiments, a Plackett–Burman design was applied to evaluate the following factors: glucose concentration (A), tryptone concentration (B), KCl concentration (C), size concentration (D), liquid volume (E), initial pH (F), temperature (G), shaking speed (H), and time (I) (Table 3). Using OD_{600} as the response value, the results (Table 4) showed that fermentation time (I), size concentration (D), and glucose concentration (A) were the significant factors affecting fermentation ($p < 0.05$).

Table 3. Plackett-Burman test design and results of *Bacillus velezensis* B313-6 culture components and conditions.

Numbers	Glucose (A)	Tryptone (B)	KCl (C)	Inoculation Amount (D)	Liquid Volume (E)	Initial pH (F)	Temperature (G)	Shaker Speed (H)	Duration (I)	OD_{600}
1	1	1	−1	1	1	1	−1	−1	−1	0.86
2	−1	1	1	−1	1	1	1	−1	−1	0.08
3	1	−1	1	1	−1	1	1	1	−1	1.09
4	−1	1	−1	1	1	−1	1	1	1	1.21
5	−1	−1	1	−1	1	1	−1	1	1	0.68
6	−1	−1	−1	1	−1	1	1	−1	1	1.05
7	1	−1	−1	−1	1	−1	1	1	−1	0.34
8	1	1	−1	−1	−1	1	−1	1	1	1.08
9	1	1	1	−1	−1	−1	1	−1	1	1.16
10	−1	1	1	1	−1	−1	−1	1	−1	0.86
11	1	−1	1	1	1	−1	−1	−1	1	1.28
12	−1	−1	−1	−1	−1	−1	−1	−1	−1	0.02

Table 4. Evaluation of the regression coefficient model coefficient of *Bacillus velezensis* B313-6 culture components and conditions and its significance test.

Source	Sum of Squares	df	Mean Square	F Value	Prob > F	Significance
	2.09	9	0.2322	36.35	0.0271	
A-Glucose	0.304	1	0.304	47.58	0.0204	*
B-Tryptone	0.0522	1	0.0522	8.18	0.1036	
C-KCI	0.0296	1	0.0296	4.63	0.1643	
D-Inoculation amount (%)	0.7356	1	0.7356	115.16	0.0086	**
E-Liquid volume (mL/250 mL)	0.0543	1	0.0543	8.5	0.1003	
F-Initial pH	0	1	0	0.0051	0.9496	
G-Temperature (°C)	0.0018	1	0.0018	0.278	0.6507	
H-Shaker speed (r/min)	0.0537	1	0.0537	8.41	0.1012	
I-Duration (h)	0.8587	1	0.8587	134.43	0.0074	**
Residual	0.0128	2	0.0064			
Cor Total	2.1	11				

Note: ** and * indicate significance at the $p < 0.01$ and $p < 0.05$ levels, respectively.

3.3.4. Steepest Ascent Experiment of *B. velezensis* B313-6

A steepest ascent experiment was conducted with the three significant factors (glucose concentration, size concentration, and fermentation time) (Table 5). The highest OD_{600} (1.27) was achieved with 2.25% glucose, 5% size concentration, and 48 h of fermentation. These conditions were used as the center point for the subsequent response surface analysis.

Table 5. Experimental design and results of the steepest climbing path of *Bacillus velezensis* B313-6.

Numbers	Glucose (%)	Inoculation Amount (%)	Duration (h)	OD_{600}
1	1.50	2	12	1.10
2	1.75	3	24	1.12
3	2.00	4	36	1.21
4	2.25	5	48	1.27
5	2.50	6	60	1.24

3.3.5. Box–Behnken Response Surface Optimization of *B. velezensis* B313-6

A Box–Behnken design was used to conduct a three-factor, three-level experiment with glucose (A), size concentration (B), and fermentation time (C) as independent variables and OD_{600} (Y) as the response variable (Table 6). Analysis of variance (ANOVA) results (Table 7) showed that the model was highly significant ($p = 0.0007$), the lack-of-fit was not significant ($p = 0.13$), and $R^2 = 0.954$ with adjusted $R^2 = 0.895$, indicating a good model fit. The regression equation was:

$$Y = 1.25 - 0.0174A - 0.0057B + 0.0208C + 0.0155AB + 0.0154AC + 0.0046BC - 0.0404A^2 - 0.0550B^2 - 0.0610C^2$$

Table 6. Box–Behnken test design and results of *Bacillus velezensis* B313-6.

Numbers	Glucose (%)	Inoculation Amount (%)	Duration (h)	OD_{600}
1	−1	−1	0	1.21
2	1	−1	0	1.13
3	−1	1	0	1.20
4	1	1	0	1.15
5	−1	0	−1	0.86
6	1	0	−1	1.00
7	−1	0	1	1.19
8	1	0	1	1.18
9	0	−1	−1	0.98
10	0	1	−1	0.88
11	0	−1	1	1.14
12	0	1	1	1.14
13	0	0	0	1.29
14	0	0	0	1.25
15	0	0	0	1.23
16	0	0	0	1.21
17	0	0	0	1.24

Table 7. Analysis of variance (ANOVA) for the response surface quadratic model.

Source	Sum of Squares	df	Mean Square	F Value	*p*-Value	Significance
Model	0.0474	9	0.0053	16.17	0.0007	***
A-Glucose	0.0024	1	0.0024	7.4	0.0298	*
B-Inoculation amount	0.0003	1	0.0003	0.7979	0.4014	
C-Duration	0.0035	1	0.0035	10.6	0.0140	*
AB	0.001	1	0.001	2.95	0.1297	
AC	0.0009	1	0.0009	2.91	0.1321	
BC	0.0001	1	0.0001	0.2587	0.6266	
A^2	0.0069	1	0.0069	21.12	0.0025	**
B^2	0.0127	1	0.0127	39.12	0.0004	***
C^2	0.0157	1	0.0157	48.1	0.0002	***
Residual	0.0023	7	0.0003			
Lack of Fit	0.0016	3	0.0005	3.48	0.1300	
Pure Error	0.0006	4	0.0002			
Cor Total	0.0497	16				

Note: $R^2 = 0.9541$, adjusted $R^2 = 0.8951$. ***, **, and * indicate significance at the $p < 0.001$, $p < 0.01$, and $p < 0.05$ levels, respectively.

The 3D response surface plots (Figure 5) showed interactions between glucose and size concentration, and between glucose and time. The optimal conditions predicted by the model were: glucose 2%, size concentration 5%, fermentation time 50 h, at which the predicted OD_{600} was 1.25.

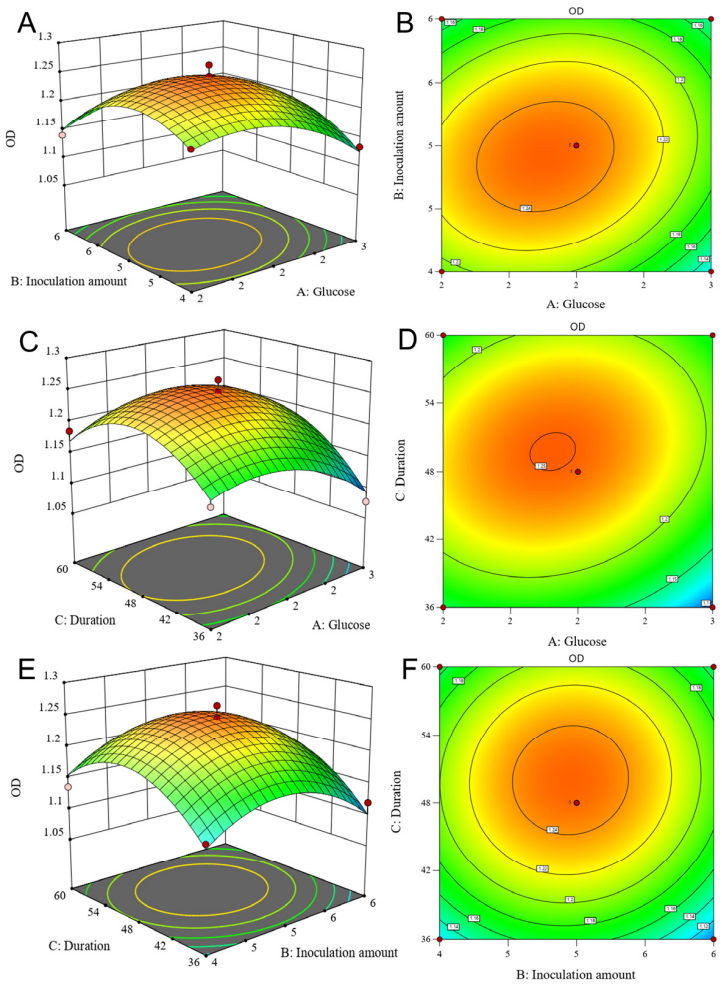


Figure 5. Response surface and contour plots showing the interactive effects of variables on OD_{600} of *Bacillus velezensis* B313-6. (**A**) Response surface of the interaction between glucose and inoculum size. (**B**) Contour plot of the interaction between glucose and inoculum size. (**C**) Response surface of the interaction between glucose and fermentation time. (**D**) Contour plot of the interaction between glucose and fermentation time. (**E**) Response surface of the interaction between inoculum size and fermentation time. (**F**) Contour plot of the interaction between inoculum size and fermentation time.

3.3.6. Validation of Optimized Conditions of *B. velezensis* B313-6

Under the predicted optimal conditions, three replicate fermentations were carried out. The measured OD_{600} was 1.24 ± 0.01, which was close to the predicted value (relative error 0.6%). Before optimization, the viable cell count was 4.0×10^8 CFU/mL, and after optimization it increased to 1.5×10^9 CFU/mL, representing a 2.7-fold increase. The inhibition rate against *C. panacicola* increased from 93.9% to 97.4% (Figure 6).

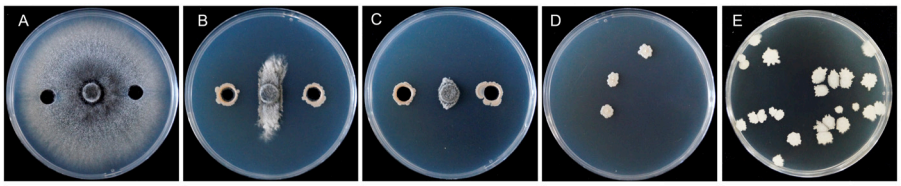


Figure 6. Comparison of the inhibition rate against *Colletotrichum panacicola* and the viable cell count of *Bacillus velezensis* B313-6 before and after optimization. (**A**) water control. (**B**) inhibition rate before optimization. (**C**) inhibition rate after optimization. (**D**) viable cell count (diluted 10^7-fold) before optimization. (**E**) viable cell count (diluted 10^7-fold) after optimization.

3.4. Field Control Efficacy and Growth-Promoting Effects

3.4.1. Control Efficacy Against American Ginseng Anthracnose

The field trial results are shown in Figure 7. All spray treatments reduced anthracnose severity to varying degrees. Ten days after the third application, the disease index of the water control was 17.63 ± 3.36. The positive control, *B. subtilis* CWP (1000 billion spores/g), achieved a control efficacy of 62.56%. *B. velezensis* B313-6 showed slightly improved efficacy with increasing dose: the low-dose treatment (33.3 mL/m^2) resulted in a disease index of 5.22 and a control efficacy of 67.60%, while the high-dose treatment (333.3 mL/m^2) resulted in a disease index of 4.60 and a control efficacy of 68.19%. Both doses of *B. velezensis* B313-6 exhibited control efficacy comparable to that of the positive control.

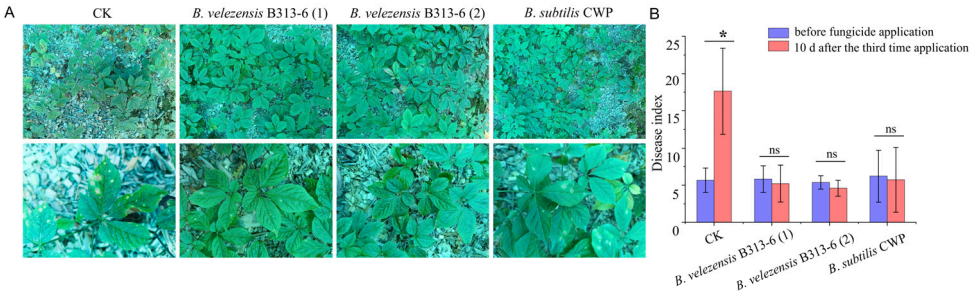


Figure 7. Field control efficacy of different treatments against American ginseng anthracnose. (**A**) Representative photographs of disease symptoms in each treatment group. (**B**) Disease index and control efficacy after the third application. Data are mean ± SD. * indicates significant difference from the water control at $p < 0.05$; ns indicates no significant difference. CK is the water control. *B. velezensis* B313-6 (1) was treated with *B. velezensis* B313-6 fermentation broth (5×10^8 CFU/mL) at 33.3 mL/m^2; *B. velezensis* B313-6 (2) was treated with the same fermentation broth at 333.3 mL/m^2; *B. subtilis* was treated with a kind of commercial wettable powder (CWP) of *B. subtilis* (1000 billion spores/g) at 0.8 g/m^2 as the positive control.

3.4.2. Growth-Promoting Effects and Rhizosphere Fungal Community Regulation

Compared with the water control, American ginseng plants treated with different biocontrol agents showed improved growth status to varying degrees (Figure 8A). Four growth indicators were determined, including plant height (Figure 8C), root length (Figure 8D), shoot fresh weight (Figure 8E), and root fresh weight (Figure 8F). The *B. subtilis* CWP used as the positive control showed growth-promoting trends, with plant height of 26.53 cm, root length of 18.03 cm, shoot fresh weight of 1.83 g, and root fresh weight of 4.81 g, corresponding to increases of 5.82%, 32.57%, 19.61%, and 24.29% over the water control, respectively. For *B. velezensis* B313-6 fermentation broth treatments, the low-dose group had a plant height of 27.50 cm, root length of 15.13 cm, shoot fresh weight of 1.69 g, and root fresh weight of 4.47 g, which were numerically increased by 9.69%, 11.25%, 10.46%, and 15.50%, respectively, compared with the water control. For the high-dose group, plant height (26.17 cm) and root fresh weight (4.24 g) showed numerical increases of 4.39% and 9.56%, respectively, while root length (13.27 cm) and shoot fresh weight (1.44 g) showed slight numerical decreases of 2.43% and 5.88%, respectively.

In terms of rhizosphere fungal community (Figure 8B), *B. velezensis* B313-6 treatment affected the relative abundance of several fungal taxa compared with the water control. The relative abundance of *Fusarium* spp., a typical soil-borne pathogenic genus, decreased numerically from 9.98% to 6.53%, while that of *Mortierella* spp., a widely recognized beneficial fungus, increased numerically from 2.95% to 5.89%.

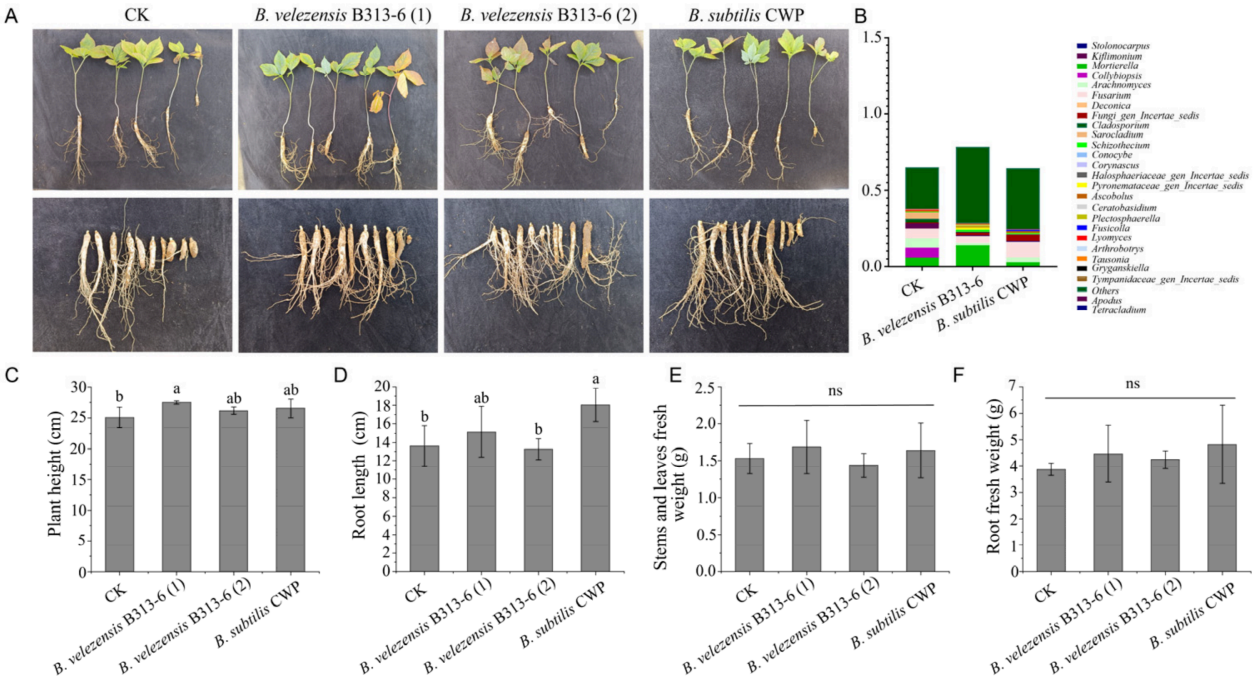


Figure 8. Effect of different treatments on the growth promotion of *Panax quinquefolius*. (**A**) Effect of different treatments on American ginseng. (**B**) Bar chart of the relative abundance of species at the genus level. (**C**) Plant height of field *P. quinquefolius* under different microbial agent treatment. (**D**) Root length of field *P. quinquefolius* under different microbial agent treatment. (**E**) Stems and leaves fresh weight of field *P. quinquefolius* under different microbial agent treatment. (**F**) Root fresh weight of field *P. quinquefolius* under different microbial agent treatment. CK is the clear water control. *B. velezensis* B313-6 (1) is treated with application of 5×10^8 CFU/mL *B. velezensis* B313-6 at doses of 33.3 mL/m2, *B. velezensis* B313-6 (2) is treated with application of 5×10^8 CFU/mL *B. velezensis* B313-6 at doses of 333.3 mL/m^2. The *B. subtilis* CWP treatment consisted of a commercial wettable powder (1000 billion spores/g) applied at 0.80 g/m^2 as the positive control. With lowercase letters indicating significant differences ($p < 0.05$), and ns means no significant difference.

4. Discussion

In this study, the strain B313-6 with strong antagonistic activity against *C. panacicola* was isolated from the rhizosphere soil of American ginseng and identified as *B. velezensis* based on morphological, physiological, biochemical, and molecular analyses (16S rRNA and *gyrA* sequencing). The *gyrA* sequence was included as an additional phylogenetic marker because 16S rRNA gene sequences alone have limited resolution for distinguishing closely related species within the *B. subtilis* group. The combination of these two markers provides robust support for the species identification. *B. velezensis* is a kind of bacterium that has been extensively studied in recent years. It has been developed into commercial biopesticides and biofertilizers, such as Kodiak® and BioYield™, both based on strain GB03, and has been used to control soil-borne pathogens and promote plant growth in various crops including cucumber, pepper, wheat, soybean, and cotton [36]. It can produce various lipopeptide antibiotics such as surfactin, fengycin, and iturin, as well as extracellular enzymes, giving it broad-spectrum antifungal activity against many plant pathogenic fungi [37,38]. The results of the antifungal spectrum assay in this study further confirmed this: *B. velezensis* B313-6 exhibited broad-spectrum antifungal activity against eight common pathogenic fungi, with particularly strong activity against *C. orbiculare*, indicating its promising biocontrol-commercial potential [39,40].

Fermentation optimization is a critical step for enhancing the yield and activity of biocontrol agents. In this study, single-factor experiments combined with response surface

methodology were used to systematically optimize the fermentation parameters of strain B313-6. The YSP medium supported better growth than LB, likely due to the rich nitrogen sources and growth factors provided by yeast extract and peptone. Glucose, inoculum size, and fermentation time were identified as the key factors influencing biomass, consistent with previous reports on *Bacillus* fermentation [41]. Notably, the initial inhibition rate of *B. velezensis* B313-6 against *C. panacicola* had already reached 93.9% before optimization, suggesting that further improvement was limited and that the inhibition rate itself was not a sensitive indicator for detecting incremental changes during the optimization process [42]. Therefore, OD_{600} was used as the primary response variable. Although the resulting increase in inhibition rate was modest (from 93.9% to 97.4%), the validation experiments confirmed that OD_{600} increases were accompanied by concurrent increases in viable cell count and antifungal activity, supporting the use of OD_{600} as a practical indirect indicator in this system. Furthermore, the Plackett–Burman design used in this study is inherently a screening tool intended to identify the most influential factors with minimal experimental effort; the reliability of the identified factors was subsequently validated through steepest ascent and response surface optimization, confirming that the screening results were effective and reproducible.

Field trial results demonstrated that *B. velezensis* B313-6 fermentation broth effectively controlled American ginseng anthracnose, with efficacy comparable to that of a commercial *B. subtilis* product used as a positive control. The similar performance between *B. velezensis* B313-6 and the commercial product suggests that *B. velezensis* B313-6 has practical applicability for field-scale disease management. Notably, the low-dose treatment (33.3 mL/m^2) performed better in promoting plant growth than the high-dose treatment (333.3 mL/m^2). High-dose treatment slightly reduced root length and shoot fresh weight, possibly due to abiotic stress or osmotic imbalance caused by excessive microbial metabolites or fermentation residues. This phenomenon has been observed in other *Bacillus* biocontrol studies [43,44], and supports the recommendation of lower application doses in practice. The decline in efficacy after the third application may reflect increased pathogen pressure in the field or limited retention time of the fermentation broth on leaves, highlighting the need for formulation development to improve leaf adherence and persistence.

Rhizosphere microbial community analysis revealed that *B. velezensis* B313-6 treatment reduced the relative abundance of *Fusarium* spp. and increased that of *Mortierella* spp. *Fusarium* is a common genus of potential pathogens in the rhizosphere of American ginseng, and its suppression may contribute to the overall disease control observed in the field. *Mortierella*, in contrast, is a widely recognized beneficial fungal genus with plant growth-promoting properties and the ability to enhance soil phosphorus availability [45]. The enrichment of *Mortierella* following *B. velezensis* B313-6 treatment suggests that the strain may indirectly promote plant growth by modulating the rhizosphere microbial community toward a more beneficial composition. This dual effect—direct antagonism against pathogens and indirect modulation of the rhizosphere microbiome—has been reported for other *Bacillus* strains, including *B. velezensis* NT35, which reduced *Fusarium* and *Ilyonectria* abundance while inducing host defense responses [22], and *B. amyloliquefaciens* FG14, which altered microbial community structure and upregulated lipopeptide biosynthesis genes [46]. Collectively, these findings suggest that *B. velezensis* B313-6 may function through a integrated biocontrol mechanism involving direct antifungal activity, rhizosphere microbial modulation, and growth promotion.

It should be noted that fermentation optimization in this study relied on OD_{600} as an indirect measure of antifungal activity, and future studies incorporating direct quantification of lipopeptides or other antifungal metabolites would further refine the optimization process. Additionally, while the field trial showed promising results, multi-year and multi-

location validation is needed to confirm the consistency and robustness of *B. velezensis* B313-6 efficacy under diverse environmental conditions. Future work should also focus on formulation development to enhance field persistence, elucidation of the molecular mechanisms underlying its biocontrol activity, and evaluation of its compatibility with existing disease management practices for American ginseng. Overall, *B. velezensis* B313-6 represents a promising biocontrol candidate with practical potential for sustainable management of American ginseng anthracnose.

5. Conclusions

In this study, *B. velezensis* B313-6 was isolated from the rhizosphere soil of American ginseng and showed strong antagonistic activity against *C. panacicola*. This strain exhibited broad-spectrum antifungal activity against several important phytopathogenic fungi. In field trials, a low dose of the fermentation broth provided effective control of American ginseng anthracnose and significantly promoted plant growth, achieving efficacy comparable to a commercial *B. subtilis* product. Notably, increasing the dose did not improve disease control and even slightly suppressed some growth traits, suggesting a threshold effect that favors lower concentrations in practical applications. Rhizosphere microbial community analysis further revealed that *B. velezensis* B313-6 treatment reduced the relative abundance of *Fusarium* spp. and increased that of *Mortierella* spp., indicating that the strain may function through a dual mechanism involving both direct antagonism and modulation of the rhizosphere microbiome. However, its colonization dynamics and interactions with native microorganisms remain to be determined. Overall, *B. velezensis* B313-6 represents a promising biocontrol candidate, though future work should focus on some commercial products, formulation development, field application strategies, and a clearer understanding of its mechanisms of action.

Author Contributions: L.L., T.H. and J.G. designed the experiments. S.F., Y.S. (Yue Shi), R.L., X.L. and N.Y. performed the experiments. S.S., Y.S. (Yuejia Song), Y.H., H.Z., and C.C. prepared the manuscripts. L.L. and J.G. checked the manuscripts. S.F., Y.S. (Yue Shi) and R.L. contributed equally to this work. All authors have read and agreed to the published version of the manuscript.

Funding: The study was supported by the Project of Development and Application of Precision Prevention and Control Technologies for Ginseng Diseases (No. SJ2025007-02), the earmarked fund for China Agriculture Research System (CARS-21), the Science and Technology Development Plan Project of Jilin Province (No. 20230202104NC), Jilin Provincial Department of Education Scientific Research Project (No. JJKH20250592KJ) and the 111 Project (No. D17014).

Data Availability Statement: The original contributions presented in this study are included in the article. Further inquiries can be directed to the corresponding author.

Acknowledgments: We are very grateful to all staff members of our team for their assistance.

Conflicts of Interest: The authors declare no conflicts of interest.

References

1. Yang, Z.; Deng, J.; Liu, M.; He, C.; Feng, X.; Liu, S.; Wei, S. A review for discovering bioactive minor saponins and biotransformative metabolites in *Panax quinquefolius* L. *Front. Pharmacol.* **2022**, *13*, 972813. [CrossRef]
2. Zhang, X.M.; Bi, Y.M.; Li, J.F.; Shao, H.H.; Jiao, X.L.; Gao, W.W. First report of root rot caused by *Fusarium armeniacum* on American ginseng in China. *Plant Dis.* **2021**, *105*, 1223. [CrossRef]
3. Jiao, X.L.; Bi, W.; Li, M.; Luo, Y.; Gao, W.W. Dynamic response of ginsenosides in American ginseng to root fungal pathogens. *Plant Soil* **2011**, *339*, 317–327. [CrossRef]
4. Liu, L.P.; Song, W.T.; Liu, R.J.; Yang, Y.T.; Zhan, H.X.; Chang, H.N.; Zhang, B.Y.; Lu, B.H.; Yang, L.N.; Gao, J.; et al. Leaf spot of *Panax quinquefolius* caused by *Colletotrichum panacicola* in northeastern China. *Can. J. Plant Pathol.* **2025**, *47*, 174–182. [CrossRef]

5. Liu, L.P.; Zhang, L.; Wang, Y.; Zhan, H.X.; Yang, J.; Peng, L.; Yang, L.H.; He, B.; Lu, B.H.; Wang, Y.; et al. Distribution, identification and characterization of *Colletotrichum lineola* and *C. panacicola* causing anthracnose on ginseng in northeast China. *Crop Prot.* **2020**, *137*, 105265. [CrossRef]
6. Yoon, M.Y.; Cha, B.; Kim, J.C. Recent trends in studies on botanical fungicides in agriculture. *Plant Pathol. J.* **2013**, *29*, 1–9. [CrossRef] [PubMed]
7. Maltby, L.; Brock, T.C.M.; Van Den Brink, P.J. Fungicide risk assess-ment for aquatic ecosystems: Importance of interspecific variation, toxic mode of action, and exposure regime. *Environ. Sci. Technol.* **2009**, *43*, 7556–7563. [CrossRef] [PubMed]
8. Alavanja, M.C.R.; Hofmann, J.N.; Lynch, C.F.; Hines, C.J.; Barry, K.H.; Barker, J.; Buckman, D.W.; Thomas, K.; Sandler, D.P.; Hoppin, J.A.; et al. Non-hodgkin lymphoma risk and insecticide, fungicide and fumigant use in the agricultural health study. *PLoS ONE* **2014**, *9*, e109332. [CrossRef] [PubMed]
9. Chien, M.Y.; Yang, C.M.; Chen, C.H. Organochlorine pesticide residue in Chinese herbal medicine. *J. Pestic. Sci.* **2022**, *47*, 30–34. [CrossRef] [PubMed]
10. Wang, Z.; Huang, L. *Panax quinquefolius*: An overview of the contaminants. *Phytochem. Lett.* **2015**, *11*, 89–94. [CrossRef]
11. Song, J.; He, Q.; Cao, K.; Song, X.; Zeng, Q. Effects of continuous cropping on soil metabolomics and rhizosphere bacterial communities in *Panax quinquefolius* L. *Front. Microbiol.* **2025**, *16*, 1698779. [CrossRef] [PubMed]
12. Bagnasco, P.; Fuente, L.D.; Gualtieri, G.; Noya, F.; Arias, A. Fluorescent *Pseudomonas* spp. as biocontrol agents againstforage legume root pathogenic fungi. *Soil Biol. Biochem.* **1998**, *30*, 1317–1322. [CrossRef]
13. Thiruvengadam, R.; Gandhi, K.; Vaithiyanathan, S.; Sankarasubramanian, H.; Loganathan, K.; Lingan, R.; Rajagopalan, V.R.; Muthurajan, R.; Iyadurai, J.E.; Kuppusami, P. Complete genome sequence analysis of *Bacillus subtilis* Bbv57, a promising biocontrol agent against phytopathogens. *Int. J. Mol. Sci.* **2022**, *23*, 9732. [CrossRef] [PubMed]
14. Zhang, P.; Xin, H.; van der Lee, T. Tree pathogens *Armillaria solidipes* influence the biocontrol activity of *Bacillus velezensis* BY6. *Biol. Control* **2023**, *179*, 105176. [CrossRef]
15. Schott, H.; Popescu, I.; Kehoe, C.; Ouangni, M.; Wareberg, E.; Avis, T.J. Cyclic lipopeptides from *Bacillus velezensis* differentially affect spore germination and cell membranes in fungal plant pathogens. *Lett. Appl. Microbiol.* **2026**, *79*, ovag035. [CrossRef] [PubMed]
16. Qi, T.L.; Sun, N.; Wei, W.; Wei, X.; Lu, J.P.; Wang, X.L.; Xie, Q.B.; Jin, P.F.; Norvienyeku, J.; Liu, W.B.; et al. *Bacillus velezensis* HAB-2 enhances rubber tree seedling growth and induces resistance to foliar diseases. *Appl. Soil Ecol.* **2026**, *221*, 106929. [CrossRef]
17. Meng, S.; Xie, C.; Dou, W.; Bao, L.; Jane, S.J.; Jin, J.; Chen, J. Mechanisms underlying the biocontrol activity of *Bacillus velezensis* TCS001 against the rice blast fungus *Magnaporthe oryzae*. *Pestic. Biochem. Physiol.* **2026**, *219*, 107022. [CrossRef] [PubMed]
18. Ahsan, T.; Chen, J.G.; Wu, Y.H.; Irfan, M.; Shafi, J. Screening, identification, optimization of fermentation conditions, and extraction of secondary metabolites for the biocontrol of *Rhizoctonia Solani AG-3*. *Biotechnol. Biotechnol. Equip.* **2016**, *31*, 91–98. [CrossRef]
19. Breig, S.J.M.; Luti, K.J.K. Response surface methodology: A review on its applications and challenges in microbial cultures. *Mater. Today Proc.* **2021**, *42*, 2277–2284. [CrossRef]
20. Hafez, M.; Rashad, Y.M.; Ibrahim, O.M.; El-Sharkawy, H.H.A.; Abd-ElGawad, A.M.; Bourouah, M.; Abdalla, S.A.; Sleem, M.M.; Madbouly, A.K. Optimization of antifungal and nitrogen-fixing activities of *Niallia circulans* YRNF1 using response surface methodology to control *Fusarium* root rot of pepper and promote the plant growth. *Rhizosphere* **2025**, *33*, 101049. [CrossRef]
21. Lou, H.X.; Luo, Q.Z.; Guo, Q.Q.; Su, R.S.; Liu, J.F.; He, H.L.; Cheng, Y.Q. Optimization of the culture medium of *Beauveria bassiana* and spore yield using response surface methodology. *Fermentation* **2024**, *10*, 587. [CrossRef]
22. Li, M.; Tang, H.; Li, Z.; Song, Y.; Chen, L.; Ran, C.; Jiang, Y.; Chen, C. Optimization of the production and characterization of an antifungal protein by *Bacillus velezensis* strain NT35 and its antifungal activity against *Ilyonectria robusta* causing ginseng rusty root rot. *Fermentation* **2023**, *9*, 358. [CrossRef]
23. Shi, Y.W.; Niu, X.X.; Yang, H.M.; Chu, M.; Wang, N.; Bao, H.F.; Zhan, F.Q.; Yang, R.; Lou, K. Optimization of the fermentation media and growth conditions of *Bacillus velezensis* BHZ-29 using a Plackett-Burman design experiment combined with response surface methodology. *Front. Microbiol.* **2024**, *15*, 1355369. [CrossRef] [PubMed]
24. Zhou, J.; Xie, Y.; Liao, Y.; Li, X.; Li, Y.; Li, S.; Ma, X.; Lei, S.; Lin, F.; Jiang, W.; et al. Characterization of a *Bacillus velezensis* strain isolated from *Bolbostemmatis Rhizoma* displaying strong antagonistic activities against a variety of rice pathogens. *Front. Microbiol.* **2022**, *13*, 983781. [CrossRef] [PubMed]
25. Chen, L.; Wu, Y.D.; Chong, X.Y.; Xin, Q.H.; Wang, D.X.; Bian, K. Seed-borne endophytic *Bacillus velezensis* LHSB1 mediate the biocontrol of peanut stem rot caused by *Sclerotium rolfsii*. *J. Appl. Microbiol.* **2020**, *128*, 803–813. [CrossRef] [PubMed]
26. Bergey, D.H. *Bergey's Manual of Determinative Bacteriology*; Lippincott Williams & Wilkins: Philadelphia, PA, USA, 1994.
27. Weisburg, W.G.; Barns, S.M.; Pelletier, D.A.; Lane, D.J. 16S ribosomal DNA amplification for phylogenetic study. *J. Bacteriol.* **1991**, *173*, 697–703. [CrossRef] [PubMed]
28. Tamura, K.; Stecher, G.; Kumar, S. MEGA11 molecular evolutionary genetics analysis version 11. *Mol. Biol. Evol.* **2021**, *38*, 3022–3027. [CrossRef] [PubMed]

29. Stackebrandt, E.; Goebel, B.M. Taxonomic note: A place for DNA-DNA reassociation and 16S rRNA sequence analysis in the present species definition in bacteriology. *Int. J. Syst. Evol. Microbiol.* **1994**, *44*, 846–849. [CrossRef]
30. Liu, T.T.; Zhang, J.Y.; Wang, T.; Li, Z.Y.; Liang, H.J.; Jiang, C.Y.; Tang, H.; Gao, J.; Jiang, Y.; Chen, C.Q. The novel *Pseudomonas thivervalensis* strain JI6 promotes growth and controls rusty root rot disease in *Panax ginseng*. *Biol. Control* **2024**, *193*, 10551. [CrossRef]
31. Wang, J.; Feng, S.; Lu, B.H.; Yang, L.N.; Wang, X.; Zhang, Y.J.; Gao, J. *Fusarium oxysporum* f. sp. *ginseng*, a new forma specialis causing Fusarium root rot of *Panax ginseng*. *Phytopathol. Mediterr.* **2022**, *61*, 417–429. [CrossRef]
32. Feng, S.; Zhang, C.; Wang, X.; Chen, C.Q.; Lu, B.H.; Gao, J. Measuring pathogenic soil fungi that cause sclerotinia rot of *Panax ginseng* using real-time fluorescence quantitative PCR. *Agriculture* **2023**, *13*, 1452. [CrossRef]
33. Chiang, K.S.; Liu, H.I.; Bock, C.H. A discussion on disease severity index values. Part I: Warning on inherent errors and suggestions to maximise accuracy. *Ann. Appl. Biol.* **2017**, *171*, 139–154. [CrossRef]
34. Piepho, H.P.; Malik, W.A.; Bischoff, R.; El-Hasan, A.; Scheer, C.; Sedlmeier, J.E.; Gerhards, R.; Petschenka, G.; Voegele, R.T. Efficacy assessment in crop protection: A tutorial on the use of Abbott's formula. *J. Plant Dis. Prot.* **2024**, *131*, 2139–2160. [CrossRef]
35. Lee, D.K.; In, J.; Lee, S. Standard deviation and standard error of the mean. *Korean J. Anesthesiol.* **2015**, *68*, 220–223. [CrossRef] [PubMed]
36. Kenfaoui, J.; Dutilloy, E.; Benchlih, S.; Lahlali, R.; Ait-Barka, E.; Esmaeel, Q. *Bacillus velezensis*: A versatile ally in the battle against phytopathogens-insights and prospects. *Appl. Microbiol. Biotechnol.* **2024**, *108*, 439. [CrossRef] [PubMed]
37. Assena, M.W.; Pfannstiel, J.; Rasche, F. Inhibitory activity of bacterial lipopeptides against *Fusarium oxysporum* f.sp. *strigae*. *BMC Microbiol.* **2024**, *24*, 227. [CrossRef] [PubMed]
38. Adeniji, A.A.; Aremu, O.S.; Babalola, O.O. Selecting lipopeptide-producing, *Fusarium*-suppressing *Bacillus* spp.: Metabolomic and genomic probing of *Bacillus velezensis* NWUMFkBS10.5. *MicrobiologyOpen* **2019**, *8*, e00742. [CrossRef] [PubMed]
39. Liu, Y.; Teng, K.; Wang, T.; Dong, E.; Zhang, M.; Tao, Y.; Zhong, J. Antimicrobial *Bacillus velezensis* HC6: Production of three kinds of lipopeptides and biocontrol potential in maize. *J. Appl. Microbiol.* **2020**, *128*, 242–254. [CrossRef] [PubMed]
40. Zhang, L.; Shao, L.Z.; Zhang, B.Y.; Li, Y.T.; Wang, Z.Y.; Song, S.H.; Yang, M.M.; Wang, B.S.; Zhai, D.D.; Liu, N.; et al. Genome analysis and secondary metabolite characterization of *Bacillus velezensis* JZ as a potential biocontrol agent. *Physiol. Mol. Plant Pathol.* **2026**, *141*, 103015. [CrossRef]
41. Cao, H.; Chen, Z.L.; Li, X.S.; Song, G.N.; Wu, Y.T.; Jin, J.; Cui, F.; Yuan, J.; Qi, H.; Wang, J.D.; et al. Optimization of fermentation conditions for *Bacillus velezensis* TCS001 and evaluation of its growth promotion and disease prevention effects on strawberries. *Biol. Control* **2024**, *198*, 105632. [CrossRef]
42. Hu, J.L.; Wang, Z.G.; Xu, W.H. Production-optimized fermentation of antifungal compounds by *Bacillus velezensis* LZN01 and transcriptome analysis. *Microb. Biotechnol.* **2024**, *17*, e70026. [CrossRef] [PubMed]
43. Wang, B.; Li, E.R.; Lin, Y.; Xiao, T.B.; Ji, X.C.; Zhao, Z.X.; Yan, W.R. Identification, biocontrol activity, and field application effect of *Bacillus velezensis* Yb-1. *Horticulturae* **2023**, *9*, 376. [CrossRef]
44. Ozimek, E.; Hanaka, A. *Mortierella* species as the plant growth-promoting fungi present in the agricultural soils. *Agriculture* **2020**, *11*, 7. [CrossRef]
45. Deravel, J.; Lemière, S.; Coutte, F.; Krier, F.; Van Hese, N.; Béchet, M.; Sourdeau, N.; Hoefte, M.; Leprêtre, A.; Jacques, P. Mycosubtilin and surfactin are efficient, low ecotoxicity molecules for the biocontrol of lettuce downy mildew. *Appl. Microbiol. Biotechnol.* **2014**, *98*, 6255–6264. [CrossRef] [PubMed]
46. Wang, J.; Wang, J.R.; Liu, T.T.; Li, X.; Gao, J.; Jiang, Y.; Chen, C.Q. *Bacillus amyloliquefaciens* FG14 as a potential biocontrol strain against rusty root rot of *Panax ginseng*, and its impact on the rhizosphere microbial community. *Biol. Control* **2023**, *182*, 105221. [CrossRef]

Disclaimer/Publisher's Note: The statements, opinions and data contained in all publications are solely those of the individual author(s) and contributor(s) and not of MDPI and/or the editor(s). MDPI and/or the editor(s) disclaim responsibility for any injury to people or property resulting from any ideas, methods, instructions or products referred to in the content.